High Rate of Antibody Secretion Is not Integral to Plasma Cell Differentiation as Revealed by XBP-1 Deficiency

This information is current as of October 20, 2015.

Nadine Taubenheim, David M. Tarlinton, Simon Crawford, Lynn M. Corcoran, Philip D. Hodgkin and Stephen L. Nutt

Supplementary Material	http://www.jimmunol.org/content/suppl/2012/08/28/jimmunol.1201042.DC1.html
References	This article **cites 39 articles**, 18 of which you can access for free at: http://www.jimmunol.org/content/189/7/3328.full#ref-list-1
Subscriptions	Information about subscribing to *The Journal of Immunology* is online at: http://jimmunol.org/subscriptions
Permissions	Submit copyright permission requests at: http://www.aai.org/ji/copyright.html
Email Alerts	Receive free email-alerts when new articles cite this article. Sign up at: http://jimmunol.org/cgi/alerts/etoc

High Rate of Antibody Secretion Is not Integral to Plasma Cell Differentiation as Revealed by XBP-1 Deficiency

Nadine Taubenheim,*,† David M. Tarlinton,*,† Simon Crawford,‡ Lynn M. Corcoran,*,† Philip D. Hodgkin,*,† and Stephen L. Nutt*,†

During B cell terminal differentiation, a complex set of transcription factors interact to drive the phenotypic and functional changes leading to the development of Ab-secreting cells (ASCs). The transcription factor X-box binding protein 1 (XBP-1) is an essential part of one of the branches of the unfolded protein response (UPR). The UPR is induced when a cell has to handle large amounts of proteins, as is the case in ASCs. Although XBP-1 was initially also ascribed an indispensable function in plasma cell development, later studies of B cell-specific deletion reported a much milder consequence of XBP-1 deficiency. Our interest was to determine whether XBP-1 was integral for the differentiation of plasma cells. Using both in vitro and in vivo assays, we found efficient generation of ASCs in the absence of XBP-1. ASCs were present at normal frequencies in resting and immunized mice and displayed a pattern of surface markers typical for plasma cells. The absence of XBP-1 resulted in a reduction but not ablation of Ab secretion and the failure to develop the cellular morphology characteristic of ASCs. Thus, XBP-1 deficiency demonstrates that the gene regulatory program controlling plasma cell differentiation can proceed relatively normally in the absence of high rates of Ig secretion. *The Journal of Immunology*, 2012, 189: 3328–3338.

T he differentiation of B cells to Ab-secreting cells (ASCs) requires the regulated interplay of several transcription factors (1). In this process, factors that sustain a B cell in an undifferentiated state, such as Pax5, are downregulated (2, 3), whereas factors promoting ASC differentiation are activated. Master regulators such as Blimp-1 or IFN regulatory factor 4 (IRF4) belong to this latter group and are responsible for repressing transcription of B cell genes or actively promoting the expression of ASC genes, respectively (4–9). X-box binding protein 1 (XBP-1) is a transcription factor also implicated in plasma cell differentiation, although its mechanism of action is less well defined (10–13). XBP-1 has a role in the unfolded protein response (UPR) that is induced when the endoplasmic reticulum (ER) is overloaded with unfolded proteins (14, 15). This may result in a translational blockade to reduce the amount of new unfolded proteins (16, 17) and an increased expression of chaperones that

facilitate protein folding (18). An inability of the UPR to resolve ER stress can further result in the initiation of apoptosis in some circumstances (18, 19). XBP-1 is a critical downstream player in the IRE1 branch of the UPR (14). After activation, the bifunctional transmembrane kinase/endoribonuclease IRE1 oligomerizes and thereby autoactivates its RNase domain. Activated IRE1 then splices out a small fragment of the mRNA transcript of XBP-1. This creates a frameshift, which generates the functional version of the XBP-1 protein, containing both a transactivation and a DNA-binding domain (14).

Plasma cells are specialized cells that are able to secrete large amounts of Ig and therefore rely on a functional UPR (15). It is thus not surprising that defective expression of XBP-1 impacts on the normal operation of a plasma cell. The role of XBP-1 in the development of plasma cells is, however, proposed to extend beyond its function in the UPR (10, 20). Although XBP-1 is expressed at a low level throughout B cell development, expression is induced dramatically during plasma cell differentiation in response to cytokines such as IL-4 (11). Early studies using chimeric mice demonstrated that the generation of plasma cells is highly impaired in the absence of XBP-1 (12). This led to the conclusion that XBP-1 is required for the differentiation of plasma cells themselves, not only for ensuring their proper secretory function. The developmental block in plasma cell differentiation of these chimeras occurred between B cell activation and terminal differentiation (12), and XBP-1 was attributed a key role in the signaling events during this process, including the upregulation of the plasma cell survival factor IL-6 (11).

In more recent studies, the generation of conditional, B cell-specific knockout mice has allowed examination of the impact of XBP-1 deficiency specifically on B cell differentiation (10, 13). These studies confirmed that XBP-1 was required for high rates of Ig secretion but surprisingly not for the formation of plasma cells. These two studies differed, however, in important aspects of their conclusions, with Todd et al. (13) concluding that XBP-1 controlled a novel developmental stage after the expression of the canonical plasma cell marker, Syndecan-1 (CD138), whereas Hu et al. (10) proposed broader functions of XBP-1 in signal transduction through

the BCR, controlling the appropriate expression of IRF4 and Blimp-1 and homing to the bone marrow niche.

We have had a long-standing interest in defining the cellular and molecular pathways involved in late B cell differentiation (1, 5, 21, 22). Thus, the purpose of the current study was to more precisely dissect the different functions of XBP-1 and to clarify whether it is involved in development of plasma cells independent of its function in UPR. Using quantitative analysis of in vitro B cell cultures, we have demonstrated a striking relationship between cell division history and ASC differentiation, with the proportion of B cells that undergo either of these differentiation events typically increasing with each consecutive division (22). In this study, we have used this quantitative approach as a tool to investigate how XBP-1 deficiency impacted on the development and function of ASCs. We find that XBP-1 plays no role in the division-linked differentiation of B cells to ASCs in vitro, in the expression of IRF4 or Blimp-1, or in the generation of plasmablasts and plasma cells in vivo. Thus, XBP-1 is not a major player in the gene regulatory network controlling ASC development. We show, however, that XBP-1 is specifically required for high-level expression of intracellular Ig and the resulting morphological changes that enable the plasma cell to secrete large amounts of Ab.

Materials and Methods

Mice

$Xbp1^{fl/fl}Cd19^{Cre/+}$ mice have been previously described (10, 13, 23), and $Xbp1^{fl/fl}Cd19^{Cre/+}$ mice were also crossed to $Blimp1^{GFP/+}$ reporter mice (7). All procedures involving animals were approved by the Animal Ethics Committee of the Walter and Eliza Hall Institute.

B cell purification and cell culture

Small resting B cells were purified out of splenic single-cell suspensions by Percoll density gradient. Naive B cells were then isolated with the B cell purification kit (MACS; Miltenyi Biotec), and for some experiments, cells were labeled with Cell Trace Violet (Molecular Probes), according to the manufacturer's protocol. Cells were cultured in B cell medium as previously described (22) and harvested at the specified time points for further analysis. Concentrations of stimuli were 20 μg/ml LPS (Sigma-Aldrich), 500 U/ml IL-4 (a gift from R. Kastelein, DNAX Research Institute, Palo Alto, CA), and 5 ng/ml IL-5 (a gift from A. Hapel, John Curtin School of Medical Research, Canberra, ACT, Australia). Mouse CD40L was expressed on the Sf21 insect cell line infected with a mouse CD40L-expressing baculovirus vector and purified as described elsewhere (24).

Immunization

For each mouse, 100 μg 4(hydroxy-3-nitrophenyl)acetyl (NP) coupled to the protein keyhole limpet hemocyanin (KLH) at a molar ratio of 17:1 was precipitated with alum and injected i.p. At the different time points post-immunization, mice were sacrificed, and spleen and bone marrow were obtained for further analysis as described previously (25).

ELISA and ELISPOT assay

Ig titers of supernatants and sera were determined by ELISA, using coating Abs and biotinylated secondary Abs from Southern Biotechnology Associates. After incubation with streptavidin–HRP (Sigma-Aldrich), the Ig concentrations were visualized with the substrate ABTS (Sigma-Aldrich). ELISPOT assays were performed on precoated Multiscreen-HA plates (Millipore). Cells were incubated on the plates for 4.5 h at 37°C. After incubation with biotinylated secondary Abs, followed by streptavidin–alkaline phosphatase (Caltag Laboratories), spots were developed using the substrate BCIP/NBT (Sigma-Aldrich). For the detection of NP-specific Abs, plates were coated overnight with NP$_1$- or NP$_{14}$-BSA (20 μg/ml). All other Abs used for coating and secondary Abs were obtained from Southern Biotechnology Associates.

Abs and flow cytometry

For intracellular flow cytometric staining, cells were washed twice with 0.1% BSA and 0.1% NaN$_3$ in PBS (staining buffer). Fixation was performed by incubation in 250 μl 2% paraformaldehyde on ice for 30 min, and cells were permeabilized by the addition of 250 μl 0.1% Tween 20 in

PBS and incubation overnight at 4°C. Cells were washed twice with staining buffer prior to staining with Abs or streptavidin conjugates on ice for 20 min. Abs used were purified and conjugated in-house: IgM (331.12; Alexa Fluor 680), IgD (11/26C; Alexa Fluor 680), IRF4 (3E4 Alexa Fluor 647), and Gr1 (8C5; Alexa Fluor 680) or obtained from BD Biosciences: Syndecan-1 (CD138)-PE (281-2), CD43-PE (S7), B220-PE-Cy7 (RA3-6B2), IgG$_1$-biotin (A85.1), and IgG$_1$-allophycocyanin (X56). For quantitative analyses, a known number of CaliBRITE beads (BD Biosciences) together with propidium iodide was added to each well before the harvest. The number of live cells per well was determined by relating the number of cells that passed through the cytometer to the number of beads that passed during the same time. Viable cells were determined by staining with Annexin V, conjugated to Alexa 647, prior to analysis together with propidium iodide. Samples were analyzed on a FACSCanto flow cytometer, and data were analyzed using the FlowJo software.

Quantitative PCR

Total RNA was prepared using a Qiagen (Hilden, Germany) RNeasy kit, and cDNA was prepared using an Invitrogen (Carlsbad, CA) SuperScript III First-Strand Synthesis System, both according to the manufacturers' protocols. Expression of all genes analyzed was quantified and normalized to expression of the housekeeping gene $Hmbs$ using the following primer sequences. The primers used for analysis of $Xbp1$ expression detected all isoforms. Primer sequences were as follows: $Xbp1$, fwd (ex2), 5′-AGC-AGCAAGTGGTGGATTTG-3′; $Xbp1$, rev (ex3), 5-CCAAGCGTGTTCT-TAACTCCT-3′; $Hmbs$, fwd, 5′-GACCTGGTTGTTCACTCCCTGAAG-3′; $Hmbs$, rev, 5′-ACAACAGCATCACAAGGGTTTTC-3′; $Cstf64$, fwd, 5′-CACCTCTGATGCAGACCTCTATCCAGGGAGG-3′; $Cstf64$, rev, 5′-CTGGGATCTGCTGCCAATGGTCCTCCTCTC-3′; Cγ1 membrane bound, 5′-GTCCTGGGCCTCAGCACAGGTCTCGTCC-3′; Cγ1 secreted, 5′-GTAGGACCAGAGGGCTCCAAGGACAC-3′; Cγ1 common, 5′-CA-CCAGGACTGGCTCAATGGCAAGGAG-3′; Cμ membrane bound, 5′-GATGAAGGTGGAGGCAGTGGTCCACAGG-3′; Cμ secreted, 5′-CAGG-TGCCGCCTGTGTCAGACATGATCAGG-3′; and Cμ common, 5′-CCCA-CAGCATCCTGACTGTGACAGAGGAG-3′.

Reactions were run and products analyzed using a Bio-Rad (Hercules, CA) C1000 Thermal Cycler.

Preparation of cells for transmission electron microscopy

Cells were pelleted in microcentrifuge tubes, the supernatant was discarded, and the intact cell pellet was fixed in 1% osmium tetroxide in PBS for 2 h. The cell pellets were rinsed three times in fresh PBS for 10 min each before being dehydrated in increasing concentrations of ethanol consisting of 10, 30, 50, 70, 90, 100, and 100% anhydrous ethanol for 15 min each step. Following dehydration, the cell pellets were infiltrated with increasing concentrations of LR White Resin (Sigma-Aldrich) in ethanol consisting of 25, 50, 75, and 100% resin for 6 h each step. After a second change of 100% resin, the cell pellets were embedded in fresh resin in gelatin capsules. The gelatin capsules were capped to exclude air, and the resin was polymerized in an oven at 60°C for 24 h.

Embedded cells in blocks were sectioned with a diamond knife on a Leica Ultracut R microtome, and ultrathin sections (90 nm) were collected onto pioloform-coated 100 mesh hexagonal copper grids. The sections on grids were sequentially stained with 2% uranyl acetate for 10 min and Triple Lead Stain for 5 min (26) and viewed in a Phillips CM120 Biotwin transmission electron microscope at 120 kV.

Results

XBP-1 deficiency does not affect B cell proliferation or survival

The amount of Ab produced following an immune response can be affected by genetic changes that influence cell behavior at numerous levels, including altering proliferation, survival, or differentiation rate. Because plasma cell differentiation is tightly linked to cell division number, we first examined the proliferation kinetics of B cells lacking XBP-1. It has been previously described that the deletion of XBP-1 in B cells does not affect cell viability and proliferation, when stimulated with LPS (13). We wanted to expand this analysis by performing a more detailed investigation of the proliferation of XBP-1 deficient B cells using different stimulation conditions and analyzing the proliferation profiles based on the distribution of cells per division. For these experiments we isolated naive B cells that were wild-type (WT), het-

erozygous ($Xbp1^{fl/+}Cd19^{Cre/+}$), or XBP-1 deficient ($Xbp1^{fl/fl}Cd19^{Cre/+}$). As expected, conditional deletion of XBP-1 in mature B cells expressing CD19-Cre was very efficient, with little residual full-length $Xbp1$ mRNA detected under all conditions tested (Supplemental Fig. 1). Stimulation of the naive B cells with CD40L+IL-4 for various times lead to comparable proliferation in

B cells deficient or heterozygous for XBP-1 as compared with WT B cells (Fig. 1A). Moreover, the cells were distributed over the same spectrum of division numbers at each of the time points, irrespective of their XBP-1 expression (Fig. 1B). Similar results were observed for cells stimulated with LPS (Supplemental Fig. 2A). Viability of the cells, as determined by the exclusion of
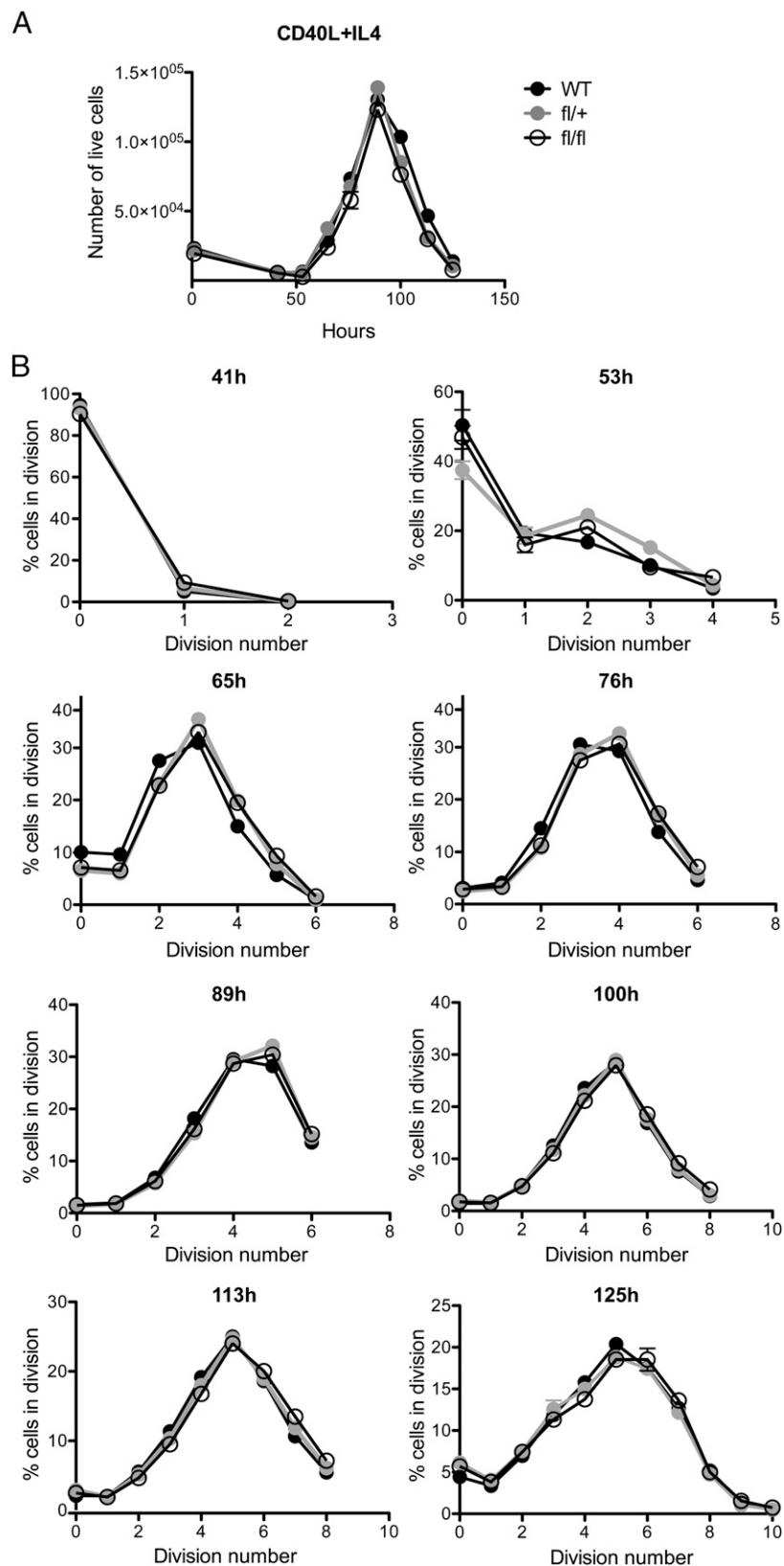
FIGURE 1. Normal proliferation in XBP-1–deficient B cells. Splenic B cells from $Xbp1^{+/+}$ (WT) and $Xbp1^{fl/+}Cd19^{Cre/+}$ (fl/+) and $Xbp1^{fl/fl}Cd19^{Cre/+}$ (fl/fl) mice were labeled with the cell tracking agent Cell Trace Violet and stimulated with CD40L+IL-4 for the indicated times. The absolute number of live cells per well at different time points (**A**) and the distribution of the cells to the different division numbers at each time point (**B**) are shown. Data shown are the mean ± SEM of three replicates per genotype per time point.

Annexin V-positive cells, was identical at the different time points (Supplemental Fig. 2B). Thus, this quantitative analysis demonstrates that neither proliferation nor survival of B cells under different stimulation conditions is affected by XBP-1 deficiency.

XBP-1 is dispensable for plasma cell differentiation in vitro

We investigated the capacity of XBP-1–deficient B cells to differentiate into plasma cells by analyzing in vitro-stimulated B cells for the expression of proteins that are linked to plasma cell differentiation. We first crossed the $Xbp1^{fl/fl}Cd19^{Cre/+}$ mice to $Blimp1^{GFP/+}$ reporter mice to detect plasmablasts that have upregulated Blimp-1 by their expression of GFP (7). Using a range of stimuli such as CD40L+IL-4+IL-5, LPS, LPS+IL-4, and CpG+IL-4 or CpG+IL-4+IL-5 (Fig. 2; data not shown), we observed little difference between B cells that lacked XBP-1 and WT B cells in the induction of Blimp-1 expression, as measured by total percentage of GFP$^+$ cells in culture or as the proportion of differentiated cells per division. This result indicates that XBP-1 is not required for the coordinated, division-linked expression of Blimp-1 in activated B cells.

Terminal B cell differentiation is further accompanied by changes in expression of many other proteins, such as upregulation of IRF4, Syndecan-1, or CD43, isotype switching and downregulation of B220. Because XBP-1 deficiency was proposed to affect IRF4 expression (10) and plasma cell development downstream of Syndecan-1 expression (13), we determined whether these changes could occur in the absence of XBP-1. To do this, we measured the expression of each of these proteins after stimulation with CD40L+IL-4+IL-5 or LPS+IL-4, conditions that strongly induce plasma cell differentiation and isotype switching in vitro. Under both conditions, the upregulation of IRF4 and the downregulation of B220 were independent of XBP-1 (Fig. 3). Similarly, isotype switching to IgG$_1$ under both stimulation conditions occurred normally in the absence of XBP-1 (Fig. 3). The proportion of Syndecan-1$^+$ cells in later divisions was reduced by ~25% in XBP-1–deficient B cells, when stimulated with CD40L+IL-4+IL-5 but not with LPS+IL-4. In contrast, CD43, a protein expressed

on terminally differentiated B cells in vitro (27), was strongly dependent on XBP-1 for its expression after stimulation with both CD40L+IL-4+IL-5 and LPS+IL-4 (Fig. 3).

Development of ASC in the absence of XBP-1

The previous results showed that, in the absence of XBP-1, the capacity of B cells to assume a plasma cell phenotype remained virtually intact. It was thus interesting to see whether in vitro-generated XBP-1–deficient Syndecan-1$^+$ cells secreted Ab at the same rate as WT cells. We sorted Syndecan-1$^+$ cells from day 4 cultures of different stimulation conditions and analyzed the proportion of IgG$_1$-secreting cells via ELISPOT. In comparison with WT, XBP-1–deficient B cells produced fewer IgG$_1$-secreting cells, and these produced ELISPOTs that were uniformly of small size (Fig. 4A, 4B). Furthermore, XBP-1–deficient B cells secreted lower amounts of IgM and IgG$_1$ when stimulated with CD40L+IL-4, CD40L+IL4+IL-5, or LPS+IL-4 (Fig. 4C).

Closer examination of the ASC population that develops after stimulation with LPS+IL-4 showed that while the proportion of cells that differentiated to IgG$_1^+$Syndecan-1$^+$ cells was comparable to WT B cells (Fig. 4D), the level of IgG$_1$ expression in this population, as detected by intracellular staining, was markedly lower in B cells that lacked XBP-1 (Fig. 4E). We investigated whether this was due to a defective splicing of Ig transcripts by analyzing the expression of the mRNA encoding the membrane-bound (m) and the secreted (s) forms of IgM and IgG$_1$ (Fig. 4F). Although the expression of the membrane-bound forms of both isotypes was independent of the presence of XBP-1, the secreted forms were reduced. This reduction was most apparent by comparing the ratio of membrane/secreted forms of IgM and IgG$_1$ (Fig. 4F).

Because the polyadenylation factor Cstf64 is required for the switch from the membrane-bound to the secreted form of IgM (28), we wanted to determine whether the reduced frequency of sIg in XBP-1–deficient B cells resulted from reduced expression of $Cstf64$. This was not the case because the expression of $Cstf64$ was if anything higher in the absence of XBP-1. The reduced amount of intracellular IgG$_1$ in XBP-1–deficient ASCs was consistent with the

**FIGURE 2.** Induction of Blimp-1 expression in WT and XBP-1–deficient B cells. B cells from $Blimp1^{+/GFP}$ mice that were either $Xbp1^{+/+}$ (WT) and $Xbp1^{fl/+}Cd19^{Cre/+}$ (fl/+) or $Xbp1^{fl/fl}Cd19^{Cre/+}$ (fl/fl) were labeled with Cell Trace Violet, stimulated in vitro under different conditions for 5 d, and analyzed by flow cytometry. (**A**) Representative dot plot of WT and fl/fl cells cultured in the indicated conditions. (**B**) Analysis of Blimp1-GFP expression based on division number. Cells were cultured in the conditions indicated on the left and gated into separate divisions according to their Cell Trace Violet intensity and percentages of GFP-positive cells determined. Data shown are the mean ± SEM of at least three replicates per genotype.
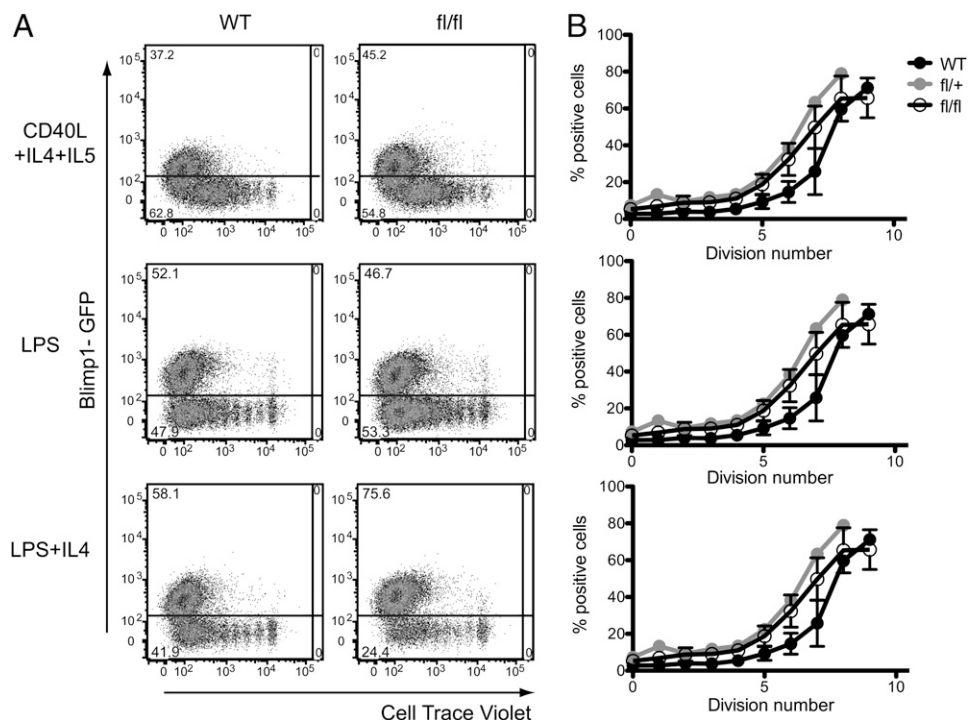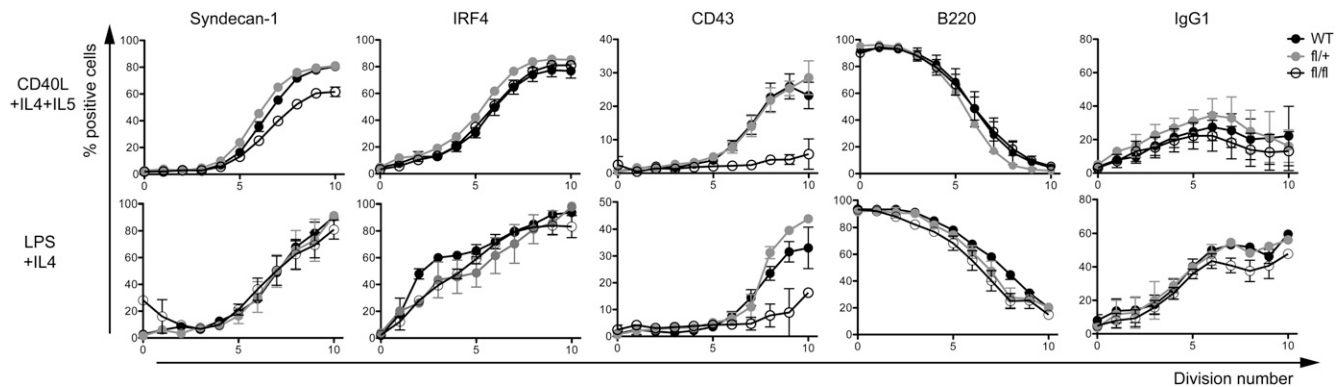
FIGURE 3. Division-linked expression changes of proteins associated with plasma cell differentiation. B cells from $Xbp1^{+/+}$ (WT) and $Xbp1^{fl/+}Cd19^{Cre/+}$ (fl/+) and $Xbp1^{fl/fl}Cd19^{Cre/+}$ (fl/fl) mice were stimulated with CD40L+IL-4+IL-5 or LPS+IL-4 for 5 d. Intracellular flow cytometry was performed to study the expression of different plasma cell–associated proteins. Cells were cultured in the conditions indicated on the left and gated into separate divisions according to their Cell Trace Violet intensity and percentages of cells positive for each marker were determined. Results shown are the mean ± SEM of at least three mice per genotype.

electron microscopic analysis of cells activated in vitro with CD40L+IL-4+IL-5 (Fig. 4G). Whereas WT B cells displayed extensive layering of the ER, which was structured around the nucleus, the density and organization of ER in XBP-1–deficient B cells was reduced.

Collectively, these data clearly indicate that the development of XBP-1–deficient ASCs is largely intact and that the principal defect in the mutant cells is impaired Ig secretion. In keeping with previous findings, Ig levels in the serum were ~10-fold decreased in $Xbp1^{fl/fl}Cd19^{Cre/+}$ mice. However, the concentrations of Ig observed were 10- to 1000-fold higher than that seen in $Rag2^{-/-}$ mice (Supplemental Fig. 3), indicating significant XBP-1–independent plasma cell development and Ab secretion.

XBP-1–deficient B cells differentiate into plasma cells in vivo

Because the in vitro activation of B cells might not reflect their full capacity to differentiate, we studied plasma cell formation in vivo in spleen and bone marrow of $Blimp1^{GFP/+}$ mice that were either WT or XBP-1 deficient. In control $Blimp1^{GFP/+}$ mice, the ASC compartment can be partitioned into Syndecan-1$^+$Blimp1-GFP^{int} plasmablasts in the spleen and Syndecan-1$^+$Blimp1-GFP^{hi} long-lived plasma cells in the spleen and bone marrow (7). Comparisons revealed no significant difference in the proportion of cells in any of these subsets with or without XBP-1 (Fig. 5A, 5B). In the absence of XBP-1, however, we consistently observed higher Syndecan-1 expression on the Blimp-1^{hi} population (Fig. 5A, histogram).

To analyze the capacity of the cells to secrete Abs ex vivo, we sorted Syndecan-1$^+$Blimp1-GFP$^+$ cells of the different subsets and determined the number of ASC, and the rate of Ig secretion per hour on a per cell basis. The total number of Igκ-secreting cells in $Xbp1^{fl/fl}Cd19^{Cre/+}$ mice did not differ significantly from WT mice (Fig. 5F), but in both splenic and bone marrow Blimp1-GFP^{hi} cells, the absence of XBP-1 caused a significant reduction in Ig κ secretion per cell (Fig. 5G). We further found significantly lower numbers of IgM- and IgA-secreting cells among the Blimp1-GFP^{hi} subset of the spleen in $Xbp1^{fl/fl}Cd19^{Cre/+}$ mice (Fig. 5C, 5E), whereas the numbers of IgG-secreting cells was significantly reduced only in the Blimp1-GFP^{hi} subset of the bone marrow (Fig. 5D). The reduced Ab secretion of XBP-1–deficient B cells was also apparent from the much smaller spots in the ELISPOT assay (Supplemental Fig. 4). Given the similar frequencies of Igκ-secreting and Blimp1-GFP$^+$ cells in control and $Xbp1^{fl/fl}Cd19^{Cre/+}$ mice (Fig. 5A, 5B, 5F), we conclude that the decreased ASC

number recorded for some Ig isotypes was the result of the very low Ig production and not an actual decrease in ASC number. In comparison, cells with intermediate Blimp-1 expression from the spleen showed a normal representation of ASCs of all isotypes and did not differ in the amount of Ig secreted per cell when XBP-1 was absent (Fig. 5C-G). These defects in Ab secretion paralleled those observed in vitro.

Because the in vitro-generated plasmablasts had abnormal ER levels, we sought to examine the ultrastructures of the different plasma cell subsets acquired ex vivo. As shown in Fig. 6A, all XBP-1–deficient cells displayed an abnormal pattern, lacking the multiple dense ER layers that were observed in WT plasma cells. All ASCs had increased amounts of cytosol, which is typical for plasma cells, but in most of the cells lacking XBP-1, large vesicle-like structures were present that were not characteristic of WT ASCs. Many of the XBP-1–deficient plasma cells contained enlarged and disorganized ER (Fig. 6B), with higher magnification revealing the presence of ribosomes around the vesicles indicative of rough ER (Fig. 6C).

To further analyze the in vivo generation of ASCs, we examined B cell differentiation during a T cell-dependent immune response by immunizing mice i.p. with the hapten NP coupled to the carrier protein KLH in alum (Fig. 7). Development of NP-specific B cells and ASCs was assessed by FACS or ELISPOT, and secretion of anti-NP Abs was measured by ELISA. At days 7 and 28, Ag-specific B cells, identified as NP-binding IgG$_1^+$B220$^+$ and negative for IgD, IgM, and Gr-1, were found in the spleen at equal frequency in WT and $Xbp1^{fl/fl}Cd19^{Cre/+}$ mice (Fig. 7A). Thus, GC-dependent expansion of NP-specific B cells was unimpaired in the absence of XBP-1. The numbers of NP-specific ASCs detected by ELISPOT did not differ in spleens from WT and $Xbp1^{fl/fl}Cd19^{Cre/+}$ mice on day 7 (Fig. 7B), suggesting a normal extrafollicular plasmablast response, but showed a significant reduction in both the spleen and bone marrow on day 28 (Fig. 7C). Affinity maturation did not seem to be affected by the absence of XBP-1, because the ratio of high-affinity anti–NP-secreting cells over total NP-specific ASCs was equivalent to the WT controls (Fig. 7D).

Once again, the most striking difference between WT and XBP-1–deficient mice was in the amount of sIg. Serum was taken from the mice on days 7, 21, and 28 after immunization, and the concentration of NP-specific IgG$_1$ was determined. At all three time points, the titers of NP-specific IgG$_1$ were significantly lower ($p < 0.005$) in $Xbp1^{fl/fl}Cd19^{Cre/+}$ sera than in control sera (Fig. 7E). This was further confirmed by analyzing the NP-IgG$_1$ secretion per
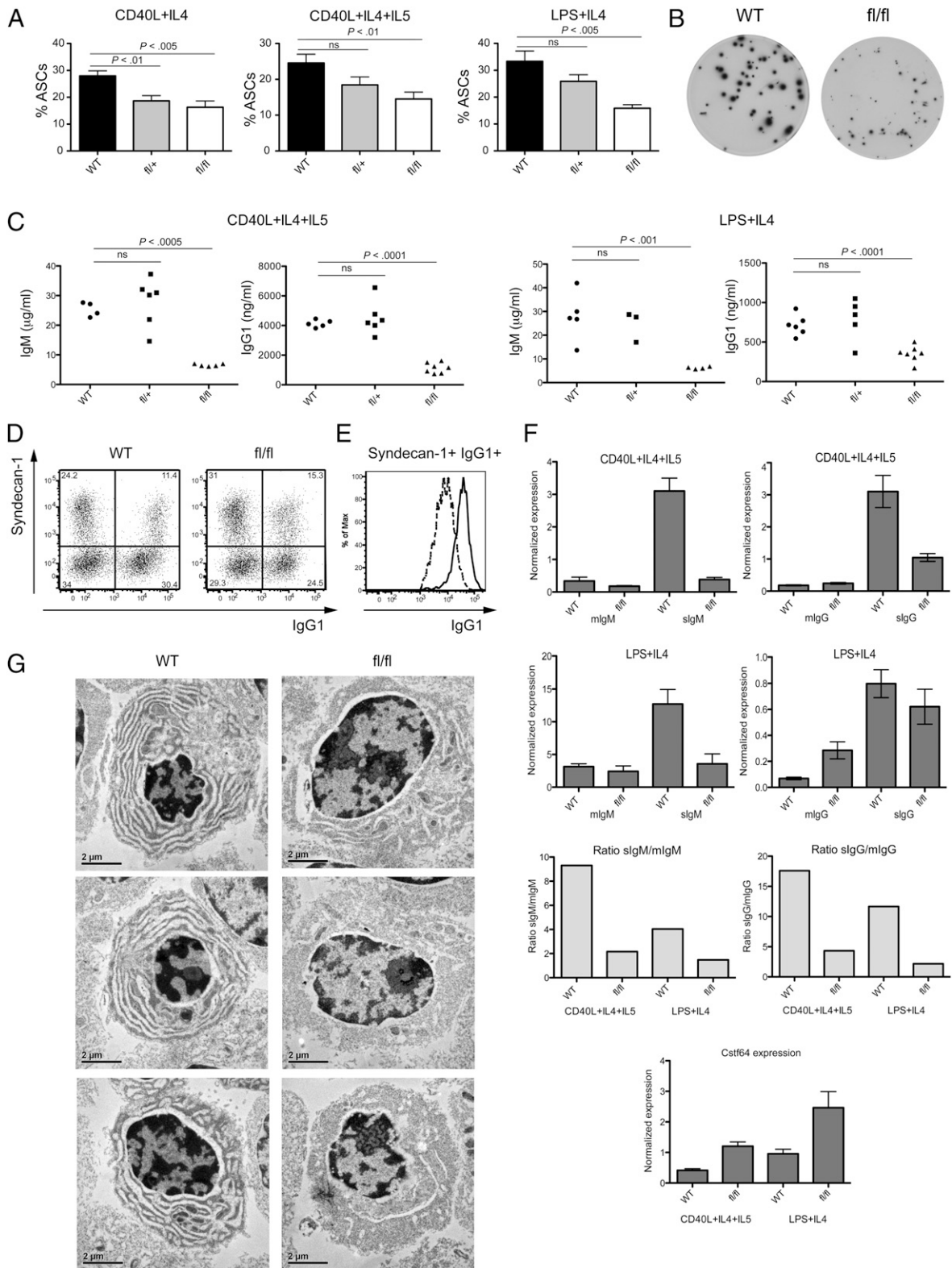
FIGURE 4. In vitro analysis of Ab secretion in XBP-1–deficient B cells. (**A** and **B**) In vitro-stimulated B cells from $Xbp1^{+/+}$ (WT) and $Xbp1^{fl/+}Cd19^{Cre/+}$ (fl/+) and $Xbp1^{fl/fl}Cd19^{Cre/+}$ (fl/fl) mice were cultured for 4 d with different stimuli before being sorted for Syndecan-1 expression and analyzed by ELISPOT for the presence of IgG_1-secreting cells. (**A**) shows the percentage of cells secreting $IgG_1 \pm SEM$ ($n = 6$), with a representative well of cells cultured in CD40L+IL-4 shown in (**B**). Original magnification ×2.7. (**C**) IgM and IgG_1 concentration in the supernatant from cells stimulated for 5 d in the indicated conditions as determined by ELISA. Each dot represents cultures derived from an individual mouse of the indicated genotypes. The p values for (**A**) and (**C**) compare the indicated genotypes using a t test. ns, $p > 0.05$. (**D** and **E**) B cells from mice of the indicated genotypes were stimulated for 4 d with LPS+IL-4 and analyzed by intracellular FACS for the expression of Syndecan-1 and IgG_1. (**E**) shows the IgG_1 expression of gated Syndecan-$1^+IgG_1^+$ cells (WT, solid line, $Xbp1^{fl/fl}Cd19^{Cre/+}$ dashed line). (**F**) Expression of the mRNA encoding mIgM and $mIgG_1$ and sIgM and $sIgG_1$ as well as expression of the polyadenylation factor $Cstf64$ were determined by quantitative PCR. RNA was generated from B cells of WT or fl/fl mice cultured for 5 d with the indicated stimuli. (**G**) Syndecan-1^+ cells were sorted from a day 5 culture with CD40L+IL-4+IL-5 and analyzed by transmission electron microscopy. Three representative cells of the indicated genotypes are shown.
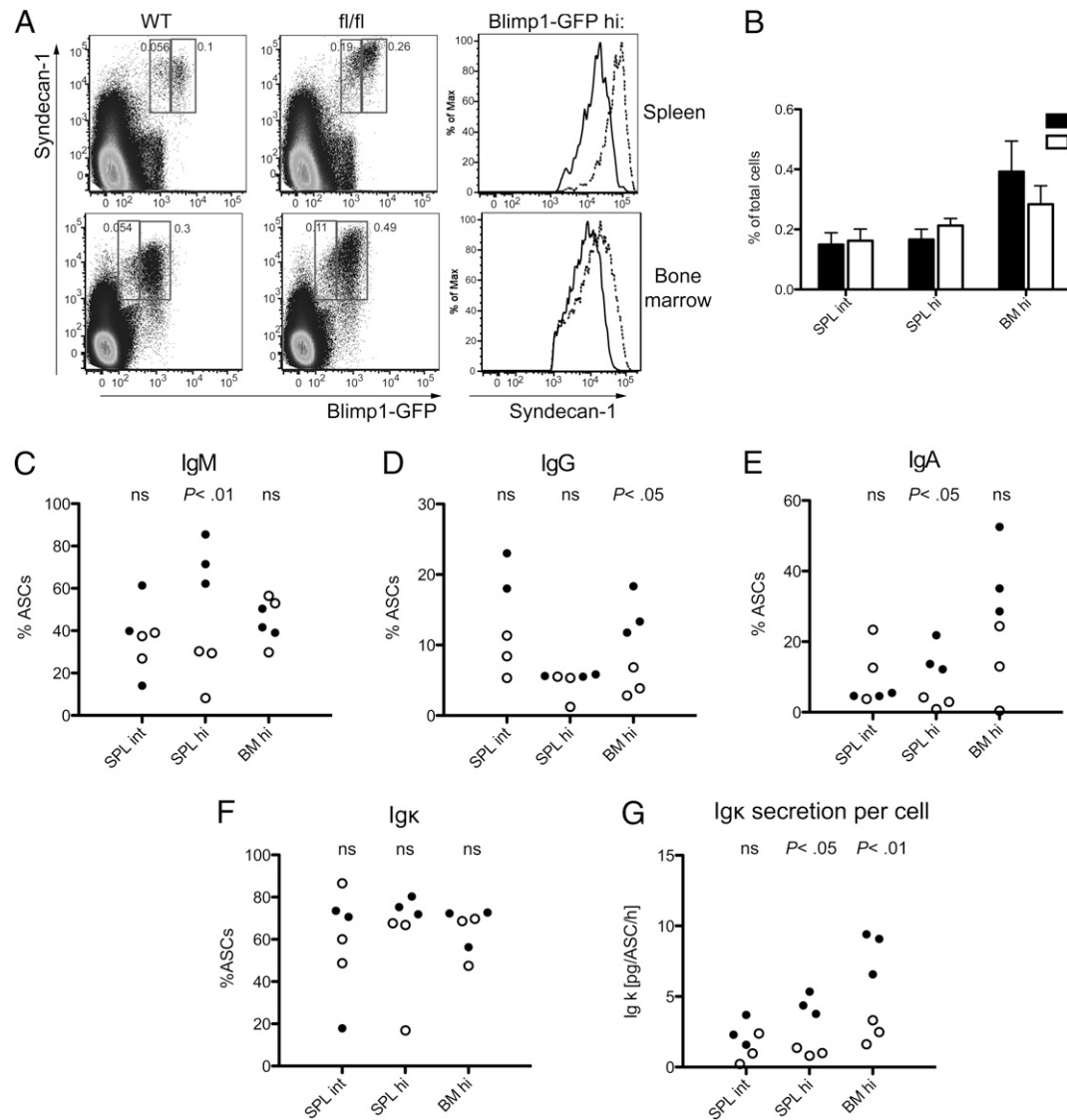
FIGURE 5.   Ex vivo analysis of XBP-1–deficient plasma cells. *Blimp1*[+/GFP] mice that were either *Xbp1*^{+/+} (WT) or *Xbp1*^{fl/fl}*Cd19*[Cre/+] (fl/fl) were analyzed for the presence of plasma cells in bone marrow and spleen. (**A**) Syndecan-1 and Blimp1-GFP expression in bone marrow and spleen (*left* and middle column). Numbers indicate the proportion of cells in each box. Histogram shows the expression of Syndecan-1 on the gated Blimp1-GFP^{hi} cells in spleen and bone marrow (WT, solid line, *Xbp1*^{fl/fl}*Cd19*[Cre/+] dashed line). (**B**) Graphs show the mean proportion of total cells ($\pm$ SEM) that were gated as Syndecan-1[+]Blimp1-GFP[int] from spleen (SPL int) or Syndecan-1[+]Blimp1-GFP[hi] from spleen (SPL hi) or bone marrow (BM hi), as shown in (A). Data was obtained from at least 5 mice per genotype. (**C–E**) Blimp1-GFP[int] and Blimp1-GFP^{hi} cells were sorted using the gates shown in (A), and the proportion of IgM- (C), IgG- (D), IgA- (E), and Igκ- (F) secreting cells was determined by ELISPOT. Each dot represents data derived from a single mouse. WT, closed circles; *Xbp1*^{fl/fl}*Cd19*[Cre/+], open circles. (**G**) The different subsets sorted as described in (C)–(F) were further investigated for the Igκ production rate per cell by ELISA. Cells of the different subsets were cultured ex vivo for 6.5 h, the supernatant was analyzed by ELISA, and the data were normalized for the number of ASCs per well as determined by ELISPOT in (F). Significance between WT and fl/fl genotypes in (C)–(F) was determined by performing a *t* test. ns, $p > 0.05$

cell. This rate was highly reduced in XBP-1–deficient ASCs on day 7 and sank below the ELISA detection level on days 21 and 28 (Fig. 7E). Thus, these in vivo studies align with our in vitro observations of XBP-1–deficient B cells. Although mutant B cells can develop and differentiate into ASCs and home to bone marrow, their capacity to secrete Ab is strongly reduced in all tissue sites.

Discussion

The aim of this study was to gain a deeper understanding of the function and importance of XBP-1 in the terminal differentiation of B cells to plasma cells. Because of the embryonic lethality of XBP-1 deficiency, the initial report on the role of XBP-1 in plasma cells used complementation of *Rag2*^{−/−} blastocysts with *Xbp1*^{−/−} embryonic stem cells to generate chimeric animals where all lymphocytes were XBP-1 deficient (12). Besides low Ig in the serum, these mice

showed a strong reduction in the number of plasma cells, pointing toward a role for XBP-1 as a key player in the transcriptional control of plasma cell development. Later studies using B cell-specific *Xbp1*-knockout mice, however, cast doubt on these conclusions because they showed the presence of XBP-1–deficient plasma cells at numbers equal to those of WT mice. The analysis of a B cell-specific *Xbp1*-knockout mouse by Todd et al. (13) revealed the normal development of Ag-specific plasma cells during the course of a T cell-dependent immune response. The numbers of Ag-specific cells and ASCs were comparable to WT mice, with reduced serum Ig levels being the only difference. These authors concluded that XBP-1 plays a role in a novel developmental stage where ASCs are Syndecan-1[+] yet have not differentiated to a high Ig-secreting stage. Conversely, Hu et al. (10) analyzed the same conditional mouse model and proposed
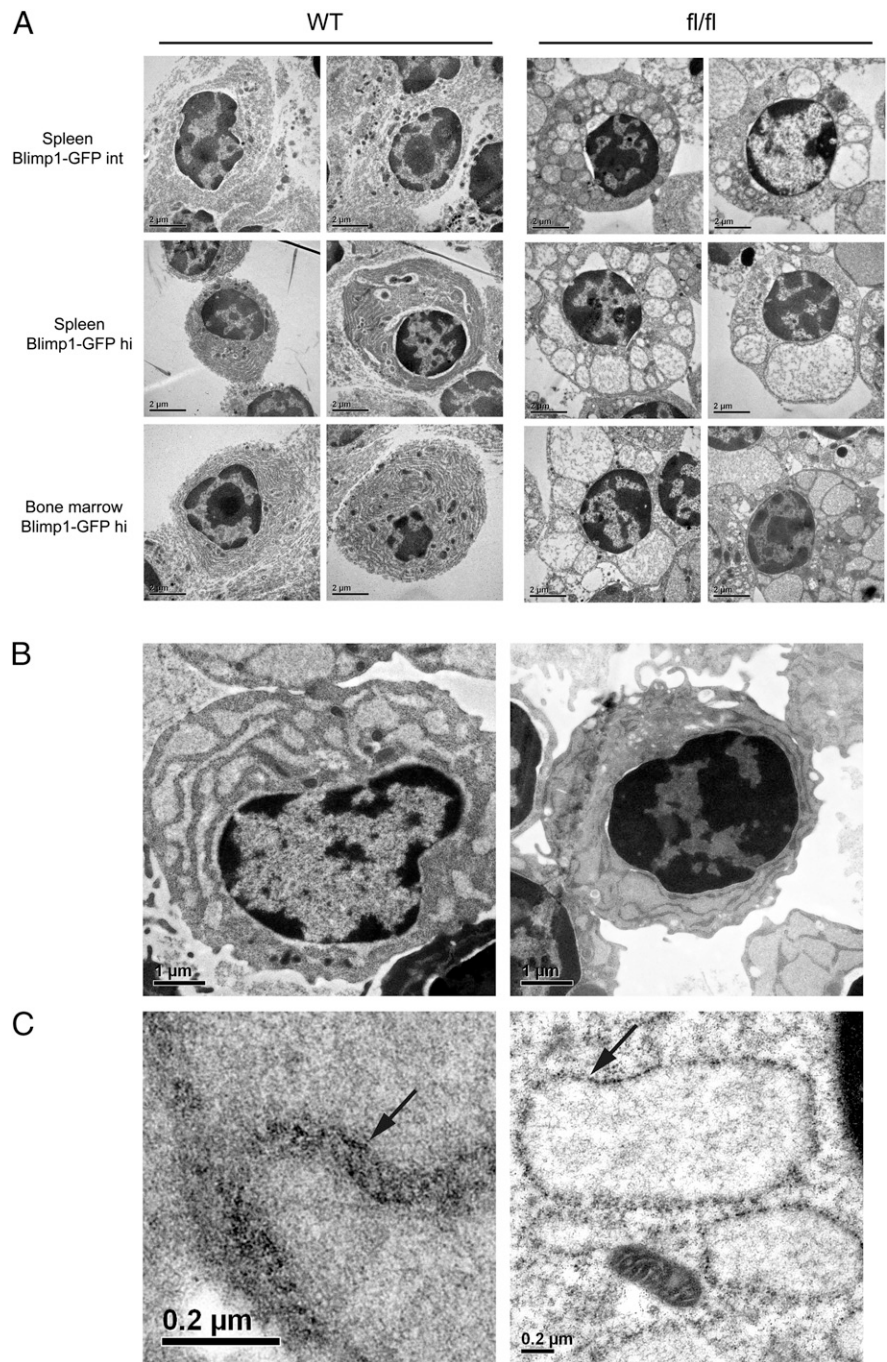
FIGURE 6. Transmission electron microscopic analysis of XBP-1–deficient plasma cells. (**A**) Syndecan-1$^+$, Blimp1-GFP^{int}, and Blimp1-GFP^{hi} cells were sorted from the spleen and bone marrow of the indicated genotypes and analyzed by transmission electron microscopy. Two representative images of each subset are shown. (**B**) shows two representative images of XBP-1–deficient plasma cells with enlarged but still recognizable ER structures. (**C**) Higher magnification of two representative images of XBP-1–deficient plasma cells shows the presence of ribosomes (arrow) around the vesicular structures, indicative of rough ER.

a more profound function of XBP-1 in the differentiation process, with XBP-1 controlling the outcome of signaling through the BCR, IRF4 expression level, and bone marrow homing. As we aim to fully understand the transcriptional program underlying the steps leading to plasma cell formation, we considered it important to refine our understanding of XBP-1. In particular, we wanted to investigate whether XBP-1–deficient B cells were not only impaired in their capacity to secrete Ig but were also affected in other ways. To answer this question, in this study, we analyzed the generation and function of plasma cells in steady-state after in vitro stimulation or after T cell-dependent immunization.

A number of proteins are differentially regulated during the development of plasma cells. We investigated whether the expression of these proteins was affected by the lack of XBP-1. Although previous studies reported stronger expression of Blimp-1 or IRF4 protein after stimulation of XBP-1–deficient B cells with LPS (10,

13), our in vitro studies revealed normal induction of these transcription factors that act both as definitive markers of ASCs and as key regulators of the differentiation process. The appropriate acquisition of IRF4 and Blimp-1 demonstrates that terminal B cell differentiation proceeds relatively normally in the absence of XBP-1. Similarly, the proportion of cells that upregulate the plasma cell marker Syndecan-1 was relatively normal. Interestingly, whereas the intensity of the Syndecan-1 expression was not different in vitro, XBP-1–deficient plasma cells in vivo showed higher expression compared with WT plasma cells. One possible explanation for this observation is that XBP-1–deficient plasma cells have altered membrane turnover kinetics because of the decreased Ig secretion rates observed.

A striking phenotypic difference we found was of the loss of CD43 expression in the absence of XBP-1 in vitro. The function of CD43 is poorly understood. It is a sialoglycoprotein expressed on
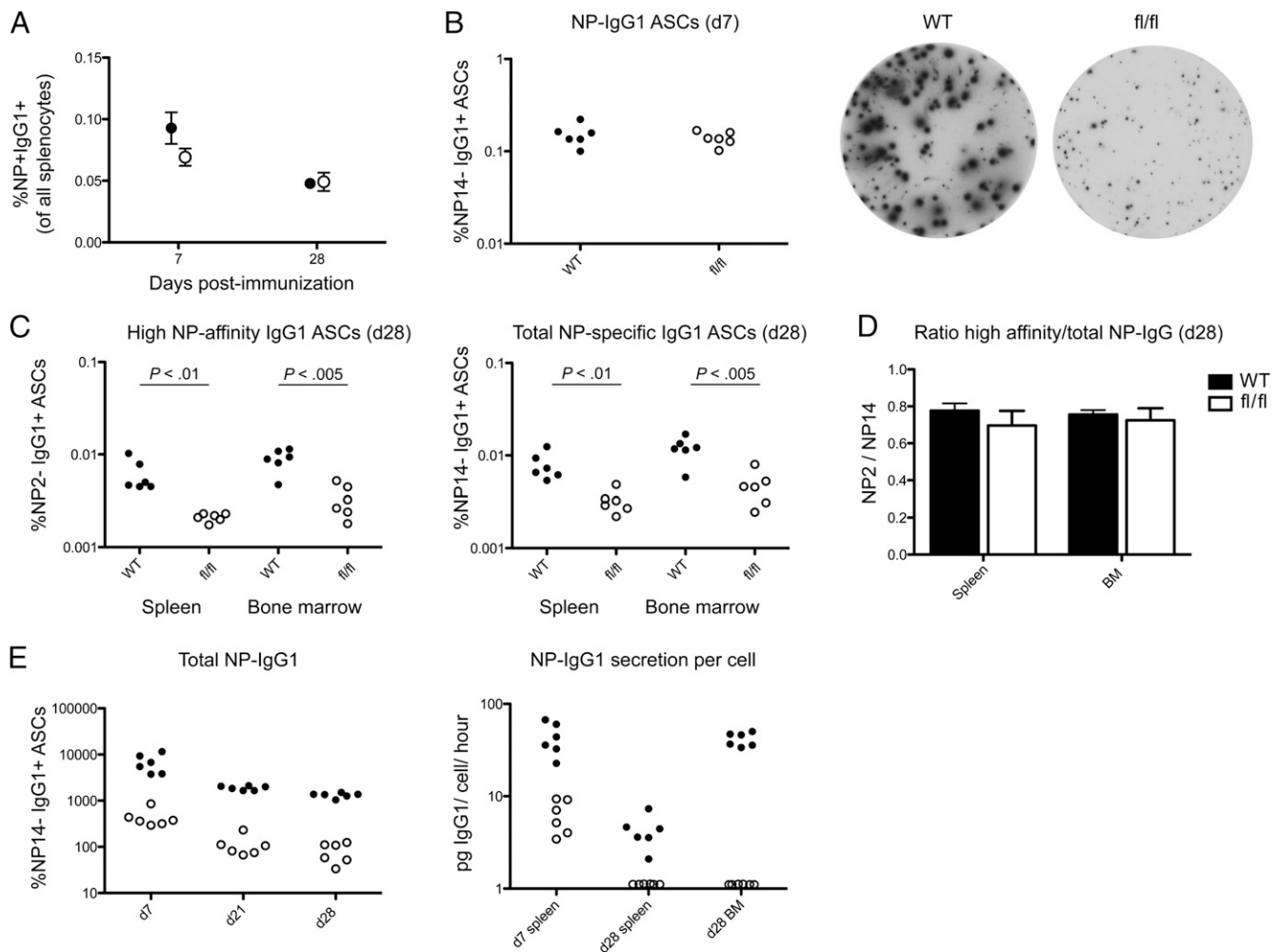
FIGURE 7. T cell-dependent immune responses in $Xbp1^{fl/fl}Cd19^{Cre/+}$ mice. $Xbp1^{+/+}$ (WT) or $Xbp1^{fl/fl}Cd19^{Cre/+}$ (fl/fl) mice were immunized with NP-KLH in alum. Mice were sacrificed on day −7 or −28 and analyzed for the proportion of $NP^+IgG_1^+$ cells in the spleens of WT (black circles) and fl/fl (open circles) mice (**A**). Data are the mean ± SEM of six mice per genotype (**B–D**). Splenocytes (days −7 and −28) as well as bone marrow cells (day −28 only) were analyzed for the presence of NP-specific IgG_1^+ ASCs by ELISPOT. ELISPOT wells were coated with either high (NP_{14}) or low (NP_2) haptenated proteins to detect total or high-affinity NP-specific IgG_1 ASCs as indicated on the graphs. The *p* values in (A) and (C) compare values from the indicated genotypes. (B) Original magnification ×3.2. (D) Affinity maturation was determined by measuring the ratio of high-affinity NP_2-IgG_1 to total NP_{14}-IgG_1. Data are the mean of this ratio ± SEM. (**E**) Serum was collected on days −7, −21, and −28, and the titer of total NP_{14}-IgG_1 was determined by ELISA. The secretion of NP_{14}-IgG_1 on a per cell basis was analyzed by cultivating splenocytes or bone marrow cells ex vivo for 6.5 h and performing ELISA of the supernatant and then normalizing the data for the number of NP_{14}-IgG_1+ ELISPOTs as determined in (B) and (C). Note the NP_{14}-IgG_1 secretion rate per cell per hour of samples from day −28 spleen and bone marrow from XBP-1–deficient were below the detection rate in this assay. Each dot is representing a single mouse. WT (black circles) and fl/fl (open circles).

most leukocytes and has been proposed to regulate proliferation and adhesion of T cells (29–31). CD43 is expressed on early developing B cells until the pre-B cell stage and is upregulated after stimulation in vitro with LPS and other stimuli (27, 32). In our in vitro studies, we found the induction of CD43 to be a terminal event in differentiation, being expressed after the induction of Blimp-1 and Syndecan-1 (data not shown). From these results, CD43 appears to be a late marker of in vitro-generated ASCs and is a potential XBP-1 target gene at this stage. However, we saw only low CD43 expression levels on plasma cells ex vivo from both the bone marrow and spleen. It is therefore unclear whether CD43 has an important function on plasma cells in vivo or whether its reduced expression on XBP-1–deficient B cells in vitro is related to the defective Ig secretion of $Xbp1^{fl/fl}Cd19^{Cre/+}$ mice.

The induction of the transcriptional repressor Blimp-1 is undoubtedly a major event in plasma cell differentiation (7–9). Using B cells from $Blimp1^{GFP/+}$ reporter mice, we saw little difference in the Blimp-1 expression between WT and XBP-1–deficient B cells

on both a population- and a division-based level (Fig. 2). In vivo, plasma cells in the spleen and bone marrow can be separated into short-lived plasmablasts and long-lived, established plasma cells, according to their increasing levels of Blimp-1 expression (7). The analysis of plasma cells in the spleen and bone marrow of naive mice or mice immunized with NP-KLH showed that the development of both Blimp1-GFP^{int} and Blimp1-GFP^{hi} cells was not affected by the absence of XBP-1. In contrast to earlier report*s* (10), our studies furthermore demonstrate that plasma cells are not dependent on XBP-1 for migration to the bone marrow. The discrepancy between the findings of Hu et al. (10) and that reported in this study are surprising because both studies used identical $Xbp1^{fl/fl}Cd19^{Cre/+}Blimp1^{GFP/+}$ mice on a C57BL/6 background. However, an important difference between the studies is that we have used T-dependent immunization to elicit an immune response from the normal polyclonal B cell repertoire, whereas Hu et al. (10) used hen egg lysozyme-specific MD4-transgenic B cells. It is conceivable that the repeated immunization of MD4 cells with

a high-affinity Ag such as hen egg lysozyme results in anergy and the reduced plasma cell homing to the bone marrow that was not observed in this study using a polyclonal response.

Both our in vitro and in vivo analyses thus show development of XBP-1–deficient plasma cells that, according to their expression of the typical surface markers, are virtually indistinguishable from WT plasma cells. In contrast, XBP-1–deficient plasma cells are functionally defective in that they secrete much less Ig and fail to remodel their ER in a manner typical of a highly secretory cell type. Thus, despite Ig secretion being the sole function of ASCs, it is not required for the relatively normal B cell terminal differentiation. Surprisingly, analysis of the transition from the mIg to sIg forms of Ig mRNA and intracellular staining for IgG$_1$ indicated that the loss of XBP-1 resulted in a defect prior to the high production of Ig. This finding agrees with the observation that XBP-1 promotes IgM synthesis (33) and is inconsistent with the idea of an accumulation of abnormal amounts of Ig in plasma cells because of the absence of XBP-1 and thus a functional UPR. How XBP-1 controls the switch to the mRNA coding for the secreted form of Ig is at present unclear. A complex of the polyadenylation factor, Cstf64 and the elongation factor ELL2 with RNA polymerase II, is known to promote sIgM and sIgG (34). At present, we have no evidence that XBP-1 directly controls the expression of either of those genes because *Ell2* is a known target of IRF4 (35) and Blimp-1 (36, 37), whereas we found that the expression of *Cstf64* was unchanged in the absence of XBP-1. Future work will address the mechanism by which XBP-1 promotes the transition from mIg to sIg.

The inability to upregulate XBP-1 in plasma cells was not without consequence because the electron microscopic analysis of XBP-1–deficient plasma cells ex vivo shows the presence of large intracellular vesicles instead of the typical structure with layers of ER. These vesicles appear to be the end product of enlarged ER structures that can be observed in many of the XBP-1–deficient plasma cells. Further evidence that the vesicles emerge from rough ER is the presence of ribosomes on their membrane, whereas the lack of a second enveloping membrane suggested that these structures were not autophagic vesicles. Given that one of the branches of the UPR is defective in XBP-1–deficient cells, it was conceivable that the ER expands as a consequence of the accumulation of large amounts of intracellular Ig. We believe that this is unlikely, because immunofluorescent confocal microscopy of the different plasma cell subsets did not reveal aberrant structures containing large amounts of Ab, when stained for IgG$_1$ or Ig κ (data not shown). Because Ig represents the vast majority of the total secreted protein in a WT ASC, one explanation is that the aberrant ER structures form as a consequence of the lack of available Ig in XBP-1–deficient cells (33). This scenario is in keeping with the previous findings that the early enlargement of the ER precedes the increased Ig production and is XBP-1 independent (38) and would explain the specific appearance of these structures in vivo, because these ASCs have a much higher Ig secretion rate than their in vitro-produced counterparts.

Although the development of plasma cells in steady-state conditions was relatively unaffected by the loss of XBP-1, we have also investigated whether XBP-1–deficient B cells showed impaired phenotypic or functional differentiation in the course of a T cell-dependent immune response. In this situation, it was possible that cells would be subject to more acute ER stress in the absence of XBP-1. Analysis of the Ab responses at early and later time points after immunization revealed that XBP-1–deficient B cells could undergo relatively normal extrafollicular and germinal center responses, as judged by the frequency of Ig class-switched Ag-binding ASCs and the normal rate of affinity maturation. Again,

the major defect was in Ig secretion, with XBP-1–deficient ASCs secreting much lower amounts of Ig on a per cell basis than WT cells. These experiments did show some loss of NP-specific ASCs at 4 wk after immunization; however, because of the lower sensitivity of ELISPOT compared with ELISA and the fact that Ab production decreases during the immune response, it is likely that this simply reflects the fact that XBP-1–deficient secretion rate had dropped below a threshold where spots could be detected and not an actual loss of ASCs.

The data presented in this paper show that XBP-1 does not function as a key transcription factor in the gene regulatory network that governs the differentiation of mature B cells into plasma cells. Although our data are broadly in agreement with that of Todd et al. (13), the conclusions differ because the authors of that study propose that XBP-1 regulates a late yet-to-be-defined stage in plasma cell differentiation that occurs after the acquisition of Blimp-1 and Syndecan-1 expression but before full Ig secretion. Although it is clear that the activation of XBP-1 is an event that is triggered by differentiation (39), we propose a different interpretation of the data, where the function of XBP-1 is predominantly, if not exclusively, enabling high Ig expression and the morphological changes that are associated with B cell terminal differentiation.

Disclosures
The authors have no financial conflicts of interest.

References

1. Nutt, S. L., N. Taubenheim, J. Hasbold, L. M. Corcoran, and P. D. Hodgkin. 2011. The genetic network controlling plasma cell differentiation. *Semin. Immunol.* 23: 341–349.
2. Neurath, M. F., W. Strober, and Y. Wakatsuki. 1994. The murine Ig 3'α enhancer is a target site with repressor function for the B cell lineage-specific transcription factor BSAP (NF-HB, Sα-BP). *J. Immunol.* 153: 730–742.
3. Barberis, A., K. Widenhorn, L. Vitelli, and M. Busslinger. 1990. A novel B-cell lineage-specific transcription factor present at early but not late stages of differentiation. *Genes Dev.* 4: 849–859.
4. Kwon, H., D. Thierry-Mieg, J. Thierry-Mieg, H. P. Kim, J. Oh, C. Tunyaplin, S. Carotta, C. E. Donovan, M. L. Goldman, P. Tailor, et al. 2009. Analysis of interleukin-21-induced Prdm1 gene regulation reveals functional cooperation of STAT3 and IRF4 transcription factors. *Immunity* 31: 941–952.
5. Kallies, A., J. Hasbold, K. Fairfax, C. Pridans, D. Emslie, B. S. McKenzie, A. M. Lew, L. M. Corcoran, P. D. Hodgkin, D. M. Tarlinton, and S. L. Nutt. 2007. Initiation of plasma-cell differentiation is independent of the transcription factor Blimp-1. *Immunity* 26: 555–566.
6. Sciammas, R., A. L. Shaffer, J. H. Schatz, H. Zhao, L. M. Staudt, and H. Singh. 2006. Graded expression of interferon regulatory factor-4 coordinates isotype switching with plasma cell differentiation. *Immunity* 25: 225–236.
7. Kallies, A., J. Hasbold, D. M. Tarlinton, W. Dietrich, L. M. Corcoran, P. D. Hodgkin, and S. L. Nutt. 2004. Plasma cell ontogeny defined by quantitative changes in blimp-1 expression. *J. Exp. Med.* 200: 967–977.
8. Shaffer, A. L., K. I. Lin, T. C. Kuo, X. Yu, E. M. Hurt, A. Rosenwald, J. M. Giltnane, L. Yang, H. Zhao, K. Calame, and L. M. Staudt. 2002. Blimp-1 orchestrates plasma cell differentiation by extinguishing the mature B cell gene expression program. *Immunity* 17: 51–62.
9. Turner, C. A., Jr., D. H. Mack, and M. M. Davis. 1994. Blimp-1, a novel zinc finger-containing protein that can drive the maturation of B lymphocytes into immunoglobulin-secreting cells. *Cell* 77: 297–306.
10. Hu, C. C., S. K. Dougan, A. M. McGehee, J. C. Love, and H. L. Ploegh. 2009. XBP-1 regulates signal transduction, transcription factors and bone marrow colonization in B cells. *EMBO J.* 28: 1624–1636.
11. Iwakoshi, N. N., A. H. Lee, P. Vallabhajosyula, K. L. Otipoby, K. Rajewsky, and L. H. Glimcher. 2003. Plasma cell differentiation and the unfolded protein response intersect at the transcription factor XBP-1. *Nat. Immunol.* 4: 321–329.
12. Reimold, A. M., N. N. Iwakoshi, J. Manis, P. Vallabhajosyula, E. Szomolanyi-Tsuda, E. M. Gravallese, D. Friend, M. J. Grusby, F. Alt, and L. H. Glimcher. 2001. Plasma cell differentiation requires the transcription factor XBP-1. *Nature* 412: 300–307.
13. Todd, D. J., L. J. McHeyzer-Williams, C. Kowal, A. H. Lee, B. T. Volpe, B. Diamond, M. G. McHeyzer-Williams, and L. H. Glimcher. 2009. XBP1

governs late events in plasma cell differentiation and is not required for antigen-specific memory B cell development. *J. Exp. Med.* 206: 2151–2159.

14. Yoshida, H., T. Matsui, A. Yamamoto, T. Okada, and K. Mori. 2001. XBP1 mRNA is induced by ATF6 and spliced by IRE1 in response to ER stress to produce a highly active transcription factor. *Cell* 107: 881–891.

15. Todd, D. J., A. H. Lee, and L. H. Glimcher. 2008. The endoplasmic reticulum stress response in immunity and autoimmunity. *Nat. Rev. Immunol.* 8: 663–674.

16. Prostko, C. R., J. N. Dholakia, M. A. Brostrom, and C. O. Brostrom. 1995. Activation of the double-stranded RNA-regulated protein kinase by depletion of endoplasmic reticular calcium stores. *J. Biol. Chem.* 270: 6211–6215.

17. Srivastava, S. P., M. V. Davies, and R. J. Kaufman. 1995. Calcium depletion from the endoplasmic reticulum activates the double-stranded RNA-dependent protein kinase (PKR) to inhibit protein synthesis. *J. Biol. Chem.* 270: 16619–16624.

18. Lee, A. S. 1992. Mammalian stress response: induction of the glucose-regulated protein family. *Curr. Opin. Cell Biol.* 4: 267–273.

19. Walter, P., and D. Ron. 2011. The unfolded protein response: from stress pathway to homeostatic regulation. *Science* 334: 1081–1086.

20. Gass, J. N., N. M. Gifford, and J. W. Brewer. 2002. Activation of an unfolded protein response during differentiation of antibody-secreting B cells. *J. Biol. Chem.* 277: 49047–49054.

21. Corcoran, L. M., J. Hasbold, W. Dietrich, E. Hawkins, A. Kallies, S. L. Nutt, D. M. Tarlinton, P. Matthias, and P. D. Hodgkin. 2005. Differential requirement for OBF-1 during antibody-secreting cell differentiation. *J. Exp. Med.* 201: 1385–1396.

22. Hasbold, J., L. M. Corcoran, D. M. Tarlinton, S. G. Tangye, and P. D. Hodgkin. 2004. Evidence from the generation of immunoglobulin G-secreting cells that stochastic mechanisms regulate lymphocyte differentiation. *Nat. Immunol.* 5: 55–63.

23. Hetz, C., A. H. Lee, D. Gonzalez-Romero, P. Thielen, J. Castilla, C. Soto, and L. H. Glimcher. 2008. Unfolded protein response transcription factor XBP-1 does not influence prion replication or pathogenesis. *Proc. Natl. Acad. Sci. USA* 105: 757–762.

24. Kehry, M. R., and B. E. Castle. 1994. Regulation of CD40 ligand expression and use of recombinant CD40 ligand for studying B cell growth and differentiation. *Semin. Immunol.* 6: 287–294.

25. Zotos, D., J. M. Coquet, Y. Zhang, A. Light, K. D'Costa, A. Kallies, L. M. Corcoran, D. I. Godfrey, K. M. Toellner, M. J. Smyth, et al. 2010. IL-21 regulates germinal center B cell differentiation and proliferation through a B cell-intrinsic mechanism. *J. Exp. Med.* 207: 365–378.

26. Sato, T. 1968. A modified method for lead staining of thin sections. *J. Electron Microsc. (Tokyo)* 17: 158–159.

27. Gulley, M. L., L. C. Ogata, J. A. Thorson, M. O. Dailey, and J. D. Kemp. 1988. Identification of a murine pan-T cell antigen which is also expressed during the terminal phases of B cell differentiation. *J. Immunol.* 140: 3751–3757.

28. Takagaki, Y., R. L. Seipelt, M. L. Peterson, and J. L. Manley. 1996. The poly-adenylation factor CstF-64 regulates alternative processing of IgM heavy chain pre-mRNA during B cell differentiation. *Cell* 87: 941–952.

29. Axelsson, B., R. Youseffi-Etemad, S. Hammarström, and P. Perlmann. 1988. Induction of aggregation and enhancement of proliferation and IL-2 secretion in human T cells by antibodies to CD43. *J. Immunol.* 141: 2912–2917.

30. Park, J. K., Y. J. Rosenstein, E. Remold-O'Donnell, B. E. Bierer, F. S. Rosen, and S. J. Burakoff. 1991. Enhancement of T-cell activation by the CD43 molecule whose expression is defective in Wiskott-Aldrich syndrome. *Nature* 350: 706–709.

31. Manjunath, N., M. Correa, M. Ardman, and B. Ardman. 1995. Negative regulation of T-cell adhesion and activation by CD43. *Nature* 377: 535–538.

32. Wells, S. M., A. B. Kantor, and A. M. Stall. 1994. CD43 (S7) expression identifies peripheral B cell subsets. *J. Immunol.* 153: 5503–5515.

33. Tirosh, B., N. N. Iwakoshi, L. H. Glimcher, and H. L. Ploegh. 2005. XBP-1 specifically promotes IgM synthesis and secretion, but is dispensable for degradation of glycoproteins in primary B cells. *J. Exp. Med.* 202: 505–516.

34. Martincic, K., S. A. Alkan, A. Cheatle, L. Borghesi, and C. Milcarek. 2009. Transcription elongation factor ELL2 directs immunoglobulin secretion in plasma cells by stimulating altered RNA processing. *Nat. Immunol.* 10: 1102–1109.

35. Shaffer, A. L., N. C. Emre, L. Lamy, V. N. Ngo, G. Wright, W. Xiao, J. Powell, S. Dave, X. Yu, H. Zhao, et al. 2008. IRF4 addiction in multiple myeloma. *Nature* 454: 226–231.

36. Shaffer, A. L., M. Shapiro-Shelef, N. N. Iwakoshi, A. H. Lee, S. B. Qian, H. Zhao, X. Yu, L. Yang, B. K. Tan, A. Rosenwald, et al. 2004. XBP1, downstream of Blimp-1, expands the secretory apparatus and other organelles, and increases protein synthesis in plasma cell differentiation. *Immunity* 21: 81–93.

37. Sciammas, R., and M. M. Davis. 2004. Modular nature of Blimp-1 in the regulation of gene expression during B cell maturation. *J. Immunol.* 172: 5427–5440.

38. van Anken, E., E. P. Romijn, C. Maggioni, A. Mezghrani, R. Sitia, I. Braakman, and A. J. Heck. 2003. Sequential waves of functionally related proteins are expressed when B cells prepare for antibody secretion. *Immunity* 18: 243–253.

39. Reimold, A. M., P. D. Ponath, Y. S. Li, R. R. Hardy, C. S. David, J. L. Strominger, and L. H. Glimcher. 1996. Transcription factor B cell lineage-specific activator protein regulates the gene for human X-box binding protein 1. *J. Exp. Med.* 183: 393–401.